

SCIENTIFIC COUNCIL OF RADIO PHYSICS, PHYSICS AND QUANTUM
ELECTRONICS

**Investigations of Temperature Sensors based on Thermosensitive
Quartz Crystal Resonators**

Summary of the PhD thesis

by

Radka Ivanova Veltcheva

**PhD Student at
Institute of Solid State Physics, Bulgarian Academy of Science**

Referee:
Prof. An. Apostolov
Dr. Kl. Brynzalov

Supervisors:
Prof. Lozan Spassov
Dr. Yu. Filippov

Sofia, 2003

GENERAL CHARACTERISTIC OF THESIS

Precise temperature measurement is an important part of modern technology. Nowadays temperature measurement and control is carrying out through a variety of methods and tools, based on different physical principles. Traditional thermocouples and platinum resistance temperature transducers (e.g. Pt100) are still dominantly used, although semiconductor based electronic thermometers would offer a much more attractive technology with respect to direct microelectronics compatibility. However, because of the wide spread variation of semiconductor parameter values, the sensitivity of semiconductor temperature sensors varies significantly from sample to sample. This means need for individual calibration and lack in interchangeability, which cause much higher cost as expected at the first glance. The disadvantages of thermocouples are the need for an accurately defined reference temperature, low sensitivity and non-linearity.

Precise thermometry, especially in the cryogenic temperature range, is compromised by the undesirable characteristics of the available sensing elements. Typical problems are nonlinearity, insensitivity, self-heating, insufficient long-term stability, low signal level and dependence on magnetic fields. All conventional possess at least one of these disadvantages.

Because of the attractive features of quartz crystal temperature sensors, as there are high sensitivity and accuracy, high dynamic range, interchangeability without recalibration, high stability, and microprocessor suiting frequency output, there have been already several attempts to develop respective measurement devices.

GOAL AND MAIN TASKS

The aim of the thesis is the creation of thermosensitive quartz crystal resonators (TSQR) as temperature sensors for measurement at wide temperature range – from 4,2K to 450K and investigations of influence of radiation environment and magnetic field at cryogenic temperatures on temperature-frequency characteristic (TFC) of TSQR.

This goal yields the following tasks:

1. to investigate acoustic characteristics of TSQR $yxbl/10^54/11^06'$ and $yxl/31^30'$ cuts at cryogenic temperatures
2. to investigate temperature-frequency characteristics of TSQR and to calculate polynomial which describes TFC with enough accuracy at wide temperature range
3. to calibrate TSQR as temperature sensors at mentioned above temperature range
4. to investigate temperature influence on activity dips phenomena
5. to investigate influence of radiation environment and magnetic fields on TFC of TSQR

Investigation methods

Number of thermosensitive quartz resonators are investigated. Experimental results of temperature-frequency characteristics, thermocycling and X-ray measurements are obtained by direct measurements of frequency, temperature, current and voltage. According to the "Temperature Measurement and Calibration" by National Physical Laboratory, Teddington Britain evaluation of the measurement uncertainty is made.

APPLICATION OF OBTAINED RESULTS

At cryogenic setup in accelerator NUCLOTRON, JINR, Dubna Russia calibrated thermosensitive quartz resonators as high precise temperature sensors for small temperature differences determination are applied.

Thermosensitive quartz resonators as temperature sensors are used in determination of selfheating of uranium under second neutron irradiation.

PUBLICATIONS

The thesis results are published in 9 reports at International scientific conferences - *14th, 15th, 16th European Frequency and Time Forum - 2000, 2001 è 2002 ã, 6th International Workshop "Relativistic Nuclear Physics from HUNDREDS of MeV to TeV"-2001ã. and 11-th National Symposium "Metrology and Metrology Assurance"-2001.*

SHORT DESCRIPTION OF THE THESIS

1. INTRODUCTION

The most important advantage of quartz is its anisotropy, allowing the design

After guaranteeing a monotonous sensor function, thermosensitive crystal cuts exhibit numerous inherent advantages as

- high sensitivity and reliability,
- immunity of the measurement signal to strong electric and magnetic fields,
- ability to function in a wide temperature range
- output of a signal, which is directly suitable for digital processing of the data

Furthermore, in contrast to most of the conventional temperature sensors, the crystal thermometers does not need a calibration of the sensitivity, because the slope of the temperature-frequency sensor function is given by the precisely controlled cut angle of the crystal plate relative to the crystallographic orientation. That is only the zero temperature vibration frequency needs to be calibrated for each sensor individually and only once for the entire lifetime of the sensor. Depending upon the desired accuracy, this can be done in an ice point or triple point of temperature reference cell.

Quartz is the only material known that possesses the following combination of properties:

- Piezoelectric
- Zero temperature coefficient cuts exist
- Stress compensated cut exists
- Low loss (i.e., high Q)
- Easy to process; low solubility in everything, under "normal" conditions, except the fluoride and hot alkali etchants; hard but not brittle
- Abundant in nature; easy to grow in large quantities, at low cost, and
- with relatively high purity and perfection.

2. TEMPERATURE FREQUENCY CHARACTERISTIC OF THICKNESS

SHARE RESONATORS

The most important advantage of quartz is its anisotropy, allowing the design of piezoelectric resonance devices, which possess either negligible or strong temperature-frequency dependence. The temperature-frequency characteristic (TFC) of each resonator can be represented by polynomial of *n-th* order and has the form of

a straight line (LC cut), quadratic (BT, CT cuts) or cubic parabola (AT, SC cuts). On this base a family of different thermostable quartz resonators for telecommunication applications has been developed. For quartz resonators with a rotated Y-cut and thickness-share mode of vibration, the resonance frequency is determined by

$$f = \frac{m}{2h} \sqrt{\frac{C_{66}}{\rho}} \quad (2-1)$$

where n is number of overtone, h -thickness of the plate, ρ - density of quartz, and

$$C'_{66} = C_{66} \cos^2 \theta + C_{44} \sin^2 \theta - C_{14} \sin 2\theta \quad (2-2)$$

C_{ij} – are elastic constants and θ the angle between the Z-axis and the main surface of the piezoelement.

Temperature dependence of frequency extremely depends on orientation of piezoelement towards the crystallographic axis of quartz. It can be expressed by polynomial in 3rd order,

$$f(t) = f_0 \left[1 + \sum_{n=1}^3 T_f^{(n)} (t-t_0)^n \right] \quad (2-3)$$

Temperature coefficients of frequency $T_f^{(n)}$

$$T_f^{(n)} = \frac{1}{n!} \left. \frac{\partial^n f}{\partial t^n} \right|_{t=t_0} \quad (2-4)$$

where $n=1,2,3$ and sum of the temperature coefficients of frequency of first, second and third order

$$T_f^{(n)} = T_f^{(1)} + T_f^{(2)} + T_f^{(3)} \quad (3-5)$$

Principal role in temperature dependence of frequency play the temperature coefficients of the elastic constants C_{ij} .

The temperature frequency characteristic of the resonator is determined by follow factors:

Primary: Angles of cut

Secondary: Overtone; Blank geometry (contour, dimensional ratios); Material impurities and strains; Mounting & bonding stresses (magnitude and direction); Electrodes (size, shape, thickness, density, stress); Drive level; Interfering modes; Load reactance (value & temperature coefficient); Temperature rate of change; Thermal history; Ionizing radiation.

According to the equation (2-3) one can see that if $T_f^{(1)}=0$ the temperature frequency characteristic possess an extremum. If $T_f^{(1)}=0$ the TFC is quadratic function and in this case, at some point $t=t_0$ the derivative of $\partial f/\partial t=0$ i.e. in narrow range the frequency change of resonator will tend to zero with respect of ambient temperature.(curve1, fig.2-1). If $T_f^{(1)}=T_f^{(2)}=0$ and $T_f^{(3)} \neq 0$ the TFC is cubic function.

In this case, in certain conditions, TFC possess inflection points and two extremums. (curve 2, fig.2-1)

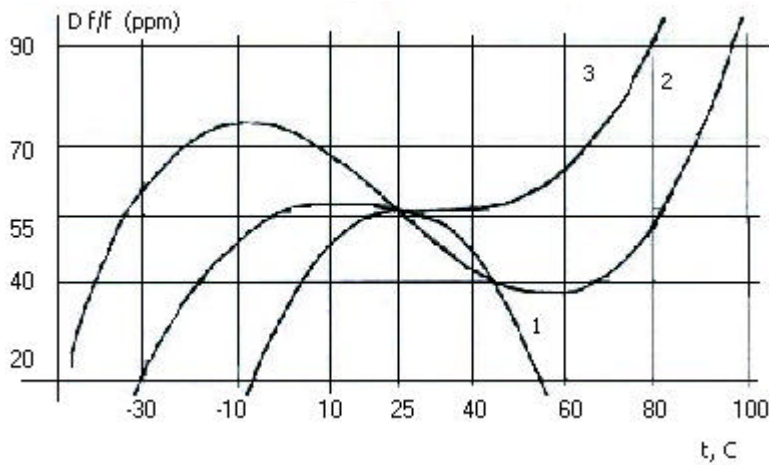


Figure 2-1

3. TEMPERATURE FREQUENCY CHARACTERISTIC OF THERMOSENSITIVE QUARTZ CRYSTAL RESONATORS AT CRYOGENIC TEMPERATURES

3.1. Temperature frequency characteristic of $yxbl/10^{\circ}54'/11^{\circ}06'$ -cut TSQR

It is well known that thermosensitive quartz resonators (TSQR) can be used as high sensitive and high precise temperature sensor for temperatures from -80°C to $+250^{\circ}\text{C}$ (190K to 520K) [3-1]. Some publications [3-2] show the interest to implement such kind of resonators as temperature sensors for cryogenic temperatures. The thesis represents some results of our investigation of TSQR in the temperature interval from 4.2K to 300K. The goal of this research was to test the possibility of using this kind of resonators as high sensitive temperature sensors for cryogenic temperatures. Moreover, we experiment with TSQR prepared and tested to measure temperatures from 220K to 450K. So we hope to extend this interval and to cover the temperatures from 4.2K to 450K with one sensor.

3.2. Experiment

The TSQR are prepared of synthetic quartz with Q -factor over $2 \cdot 10^6$ on $yxbl/10^{\circ}54'/11^{\circ}06'$ -cut plates. The resonators are hermetically sealed using thermoresistive welding in standard capsules of HC-18U type (dimensions $13.5 \times 11 \times 4.6$ mm), filled with helium (fig.3-1).

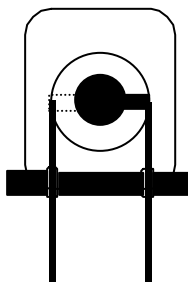


Figure 3-1

The basic problems we solved when testing TSQR at cryogenic temperatures were:

- How to obtain cryogenic temperatures below to 4.2K?
- How to excite the TSQR using quartz generator with TSQR outside of the electronic circuit?
- How to measure the frequency and the temperature of the TSQR simultaneously?
- How to save the measured data for further observation and analysis?

To answer all these questions experimental equipment was assembled which is schematically shown on fig.3-2. The equipment has two versions. One for measurement of temperatures from 77K to 300K where the coolant is liquid nitrogen and an other for temperatures from 4.2K to 300K using liquid helium. The liquid gases are saved in special containers. The temperature at the top of the container is 300K (room temperature) and lightly drops to 77K (4.2K) at the liquid surface. So to put the resonators at different temperatures it is necessary to move them vertically inside the container. For this purpose a special stock is designed. A copper shield thermally isolates its head where two resonators and a calibrated temperature sensor having good thermal contact are installed.

The TSQR are connected by means of coordinated coaxial cables to special quartz generators (QG) and excited on 3-th overtone at 26.5 MHz. The connection between the QG and the TSQR is fine balanced. The output of the QG represents a sinusoidal analogue signal with high short time stability (about $1 \cdot 10^{-8}$).

The output signals of the QG are measured using high precise frequency counters supplied with IEEE-488 interface to personal computer(PC). To obtain the reference temperature a calibrated thermoresistor is used, which current and voltage are measured by picoammeter and microvoltmeter respectively.

The data measured is send to the personal computer (PC) every second. The PC computes the temperature (on the base of the calibration data and the measured current and voltage data), saves the frequency and temperature data in files on a hard disk and shows their values as graphics on the PC screen. The graphics represent the course of the temperature and the frequency in chosen time interval, 10 minutes usually.

Having this equipment the experiment is carried out as follows. First the stock with the mounted thermoresistor and resonators in its head is placed at the top of the container. In a short time the temperature of the head obtains the temperature of the gas at this place. Then the stock is some millimeters moved down. Again for some minutes the resonators and the thermoresistor obtain the temperature of the gas at this point. So with slowly movements and waitings the head of the stock reaches the liquid gas. Then this procedure is repeated but the movements are in the reverse direction. During this time the temperature and the frequency are measured simultaneously.

More than 200 resonators are tested at cryogenic temperatures. Some of them are measured two or three times below to nitrogen and helium temperatures.

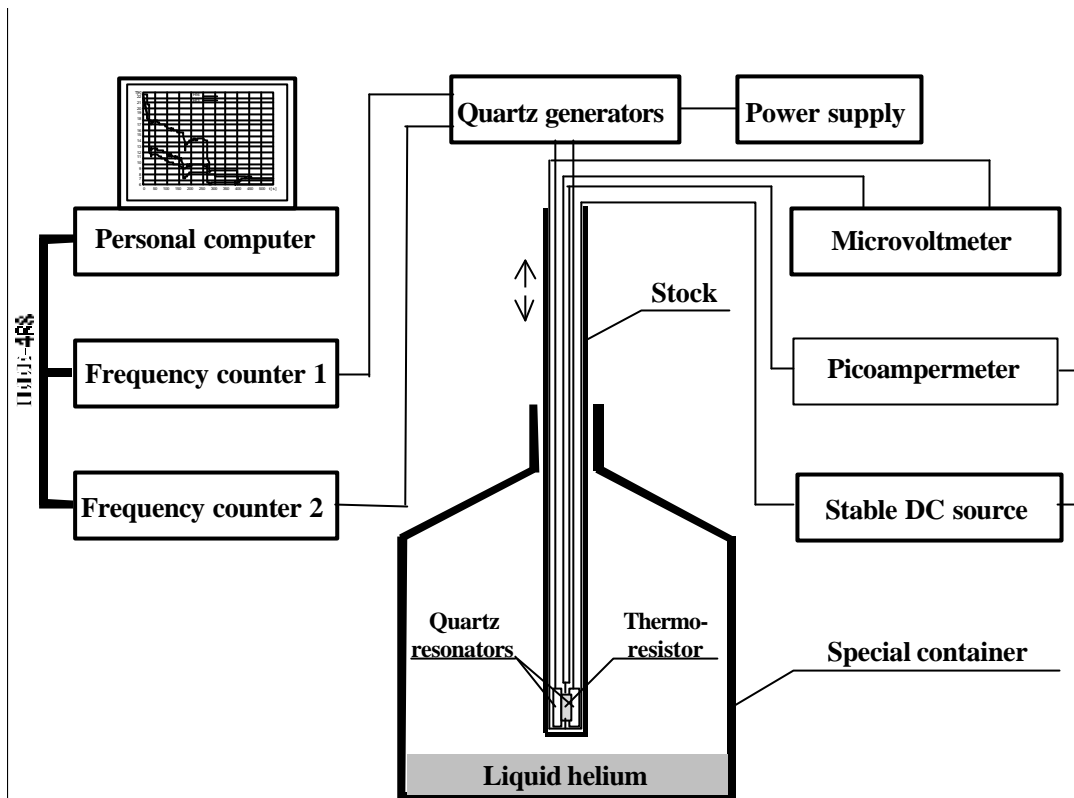


Figure 3-2

3.3. Analysis

For the analyses of this big amount of experimental data a computer program is designed. Some of its functions are listed below.

1. Display of the experimental data. This function restores the graphics as they are during the experiment and allows observing the pictures in details. So some fine instabilities of the resonators behaviour were found.
2. Creation of temperature-frequency characteristics (TFC). This is the main function of the analyses. TFC can be prepared for different temperature intervals for different resonators.
3. Approximation of the data and the TFC using some mathematical functions. To calculate TFC we approximate the obtained temperature data using exponent function or other functions. The approximation of the TFC allows finding the temperature sensitivity of the resonator.
4. Elimination of wrong data. During the experiment casual apparatus errors input wrong frequency or temperature data. The software allows to remove such kind of errors.
5. Hardcopy of the graphics. This is a very useful function when showing and archiving data. The so prepared pictures can be inserted in text documents.

3.4. Results

The experience of more than two years of experiments and the analyses of the measured data can be generalised as follows.

1. In the temperature interval from 4.2K to 130K the TFC of all resonators are non-linear monotonous increased functions (fig.3-3a). In this interval the sensitivity increases with the increase of the temperature starting with a value of about 2Hz/K at 4.2K. Over 130K the TFC has linear character and the sensitivity is

about 1000Hz/K. Typical TFC for the temperature interval from 4.2K to 300K is shown on fig.3-3b. The TFC in all temperature intervals are good approximated with polynomial of 3-th degree. Other measurements and analyses [3-3] show that the resonators keep their sensitivity and the linearity of their TFC to temperatures of about 500K.

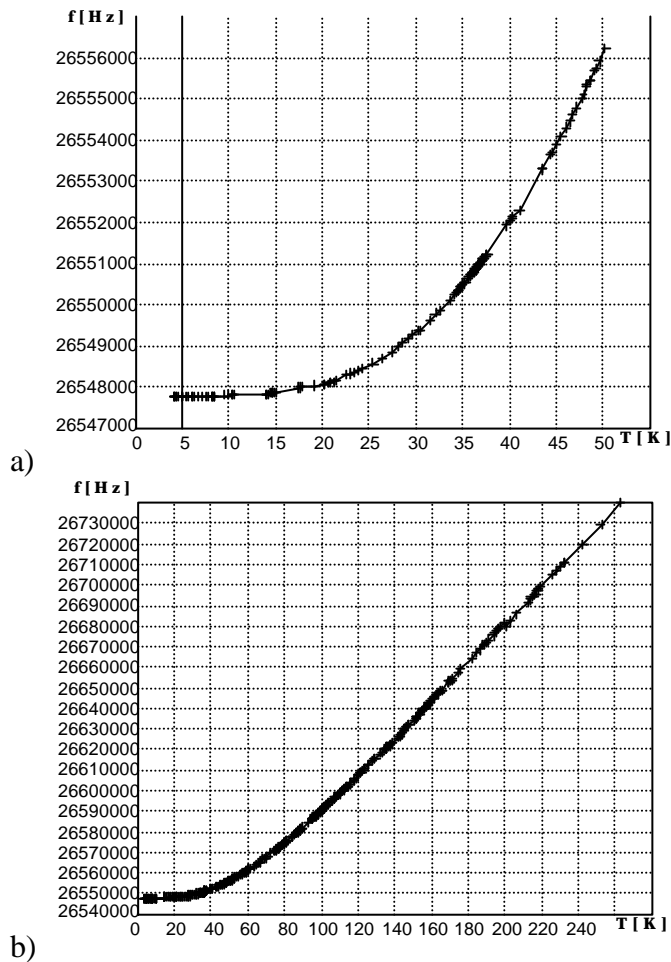
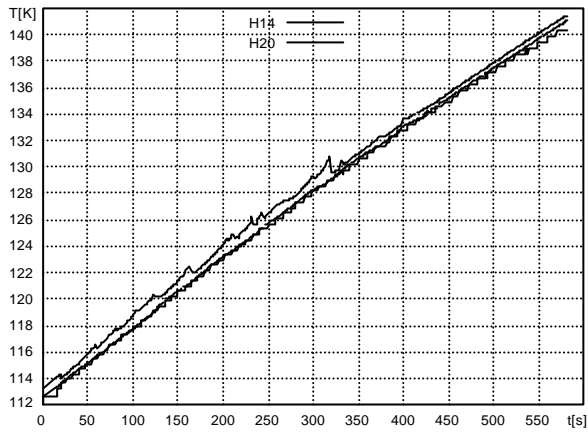


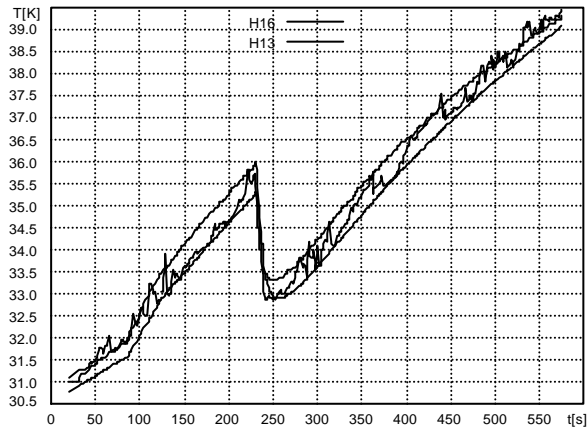
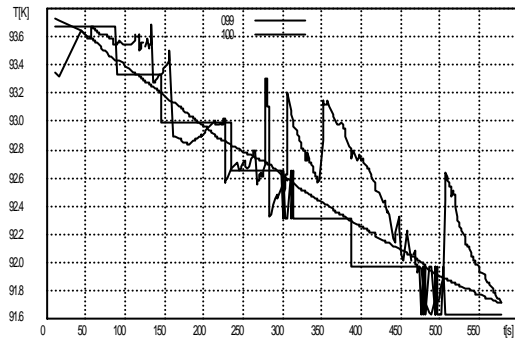
Figure 3-3

2. For some of the resonators in particular temperature intervals (from 90K to 110K and from 120K to 135K) different disturbances and instabilities were registered:
 - increase of the noise level (fig.3-4a);
 - fluctuation of the frequency when the temperature only increases or decreases (fig.3-4b);
 - frequency jumping (fig.3-4c);
 - stopping of the resonator (fig.3-4d).

It is interesting to note that in most of the cases of instability when putting the resonator at same temperature the disturbance disappears. This is possible when the time between the two measurements is within a few days. When this time is more than a week the instability can be observed again.



a)



c)

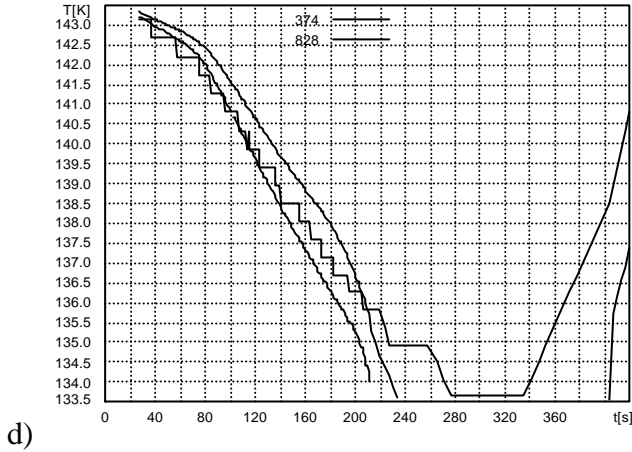


Figure 3-4

The most possible reasons of these instabilities are:

- the influence of the resonator's holders;
- the presence of residual impurity gases in the capsules;
- the excision of other mode and type of vibrations at some temperatures.

Because of the different temperature coefficients of the quartz and the holder's metal it is possible the presence of tension between the holder and the crystal. The same situation is possible at the interface between the quartz plate and the resonator's electrodes.

When other gases except helium present in the resonator's capsule they can condense or freeze on the crystal's surfaces at some temperatures and this way disturb the vibrations of the plate.

The change of the elastic constants and the dimensions of the quartz plate with the change of the temperature may cause excitation of other mode and type of vibrations. Our investigations will be focused on this problem because of its importance.

3.5. Temperature frequency characteristic of $yx1/-31^\circ 30'$ -cut TSQR

Miniature resonator with $yx1/-31^\circ 30'$ cut quartz plate on the fundamental frequency 29,3 MHz have been made. The diameter of the plate is 5 mm and its thickness is 0.083 mm. After it has been polished silver electrodes with 1.9 mm diameter have been deposited on the main surfaces of the plate. The thickness of electrodes vary from 500 Å to 1200 Å. Piezoelements are enclosed in a standard HC – 45U crystal enclosure and filled with dry nitrogen or helium.

A polynomial of third order that describes temperature frequency characteristic with enough accuracy at temperature range from 4,2K to 300K.(Fig.3-5).

$$f(t) = -0.0059t^3 + 4,8867t^2 - 167,99t + 28844900$$

The coefficients of the polynomial are $K_f^{(1)} = -5,9 \cdot 10^{-3}$; $K_f^{(2)} = 4.8867$; $K_f^{(3)} = 167.99$.

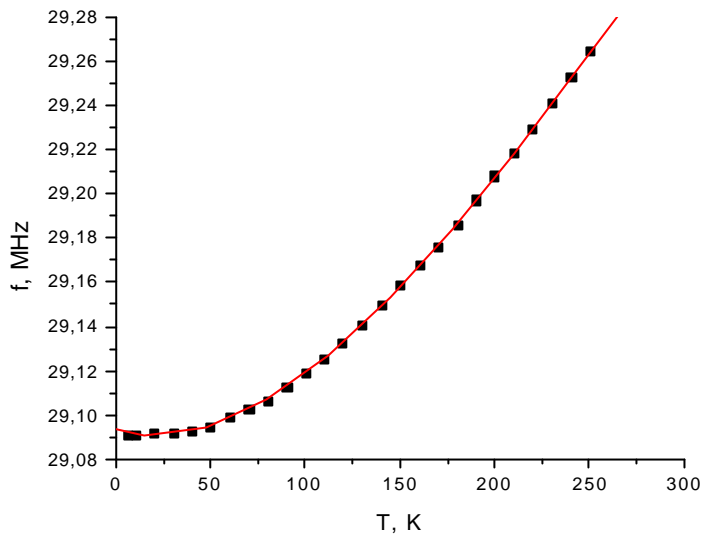


Figure 3-5

Temperature-frequency characteristic at the temperature range below 40K to the temperature of liquid helium (4,2K) can be described better by follow equation:

$$f(t) = -1.0185 t^3 + 2.6932 t^2 - 47.27 t + 28844200$$

as it is shown on Figure 3-6.

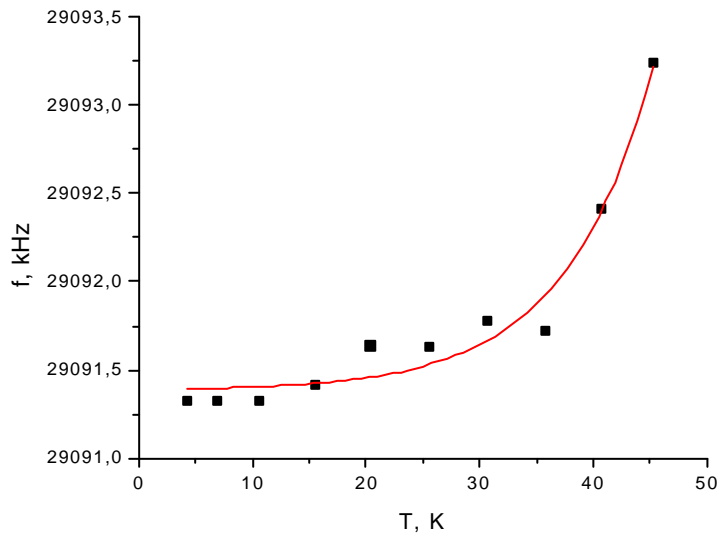


Figure 3-6

In the temperature interval from 4,2 K to 130 K the TFC of the resonators are monotonous increasing function. In this interval the sensitivity increases with the increasing of the temperature starting with a value of about 2 Hz/K at 4,2K to a value of 900 Hz/K at 130 K. Over 130 K the TFC has linear character and the sensitivity is about 1000 Hz/K

One of the advantages of TSQR as temperature sensor is its high temperature sensitivity. It is different for different temperature range:

2 Hz/K at 4,2 K (temperature of liquid helium),

60 Hz/K at 20 K,

750 Hz/K at 77,3 K (temperature of liquid nitrogen),

900 Hz/K at 130 K,

1000 Hz/K at 300 K,

This allows the measurement of the temperature fluctuations

at 4,2K, $\Delta T_{\min} = 50\text{mK}$,

at 20 K, $\Delta T_{\min} = 8 \text{ mK}$,

at 130 K, $\Delta T_{\min} = 0,12 \text{ mK}$,

at 300 K, $\Delta T_{\min} = 0.085 \text{ mK}$.

This microdegree sensitivity allows measuring frequency deviation of units in 10^9 , however, for sensitivity higher than 10^{-4} K is limited by measuring equipment.

In particular temperature intervals [90-110]K and [120-135]K the some disturbances of the behaviour of some of the resonators are observed, as it was mentioned in previous section.

4. DISTURBANCES IN TEMPERATURE FREQUENCY CHARACTERISTIC OF TSQR AT CRYOGENIC TEMPERATURES

As it was mentioned above there are some disturbances in temperature frequency characteristic of the resonators. TFC is linear function, the sensitivity is about 1000Hz/K, but some disturbances are appeared at temperature range [90-110]K and [120-135]K. These disturbances are due to possible acoustic coupling between main and spurious modes, which have different temperature sensitivity. This phenomenon is called “activity dips”.

Activity dips (jumps) in the frequency temperature response of quartz resonators were previously studied by LCEP, ENSMM, Besancon, France through combined analytical and numerical modellings. It is necessary to validate preliminary simulations, since electrical output behaviour is not sufficient to clearly identify the thermo-dependent couplings, which are known to provoke activity dips. FEM simulations are required whenever the spurious modes involved have a too complicated structure to be analytically modelled. Due to limitations in quartz material characterization, differences are expected between predicted and observed temperature of activity dips.

5. INVESTIGATIONS OF MODE COUPLING (ACTIVITY DIP) IN NLC-CUT TSQR BY FINITE ELEMENT METHOD ANALYSIS

The present chapter proposes a systematic modal analysis performed with finite element program about thermo-sensitive resonators in NLC cut of quartz [5-1] over a large temperature range. The analysed design consists of small diameter flat parallel, mass-loaded resonators operating on fundamental overtone 29.3 MHz. We present a description of the influence of several factors on the stability of the mode pattern along temperature variations down to low temperatures.

Some papers [5-2,5-3] have already been devoted to the use of Finite Element Analysis (FEA) for the understanding of activity-dip phenomenon in quartz resonators. The efficiency of FEA in this field mainly depends on the accuracy of material constants and on the possibility to simultaneously fit the actual mode shapes of the mode of interest and the involved spurious modes with a single set of generic interpolating functions while keeping the size of matrix problem as reasonable as possible. The purpose of here-presented study was not to track with the best possible accuracy the activity-dips expected in a given and stable design of thermo-sensitive quartz resonator (TSQR), but to give suggestions for possible optimisation of a new design, characterised by rather small dimensions (Fig.5-1) and operating in fundamental thickness mode in so-called NLC orientation [5-1]. For this singly rotated cut of quartz ($\phi=0$, $\theta=-31^{\circ}30'$), a electric field along the thickness of plate drives only the B-modes, which have then a pure u_I polarisation, as have C-modes in AT cuts. From the point of view of finite element analysis (FEA) operation on fundamental mode is expectedly easier to model than operation on higher overtone since only one layer of elements with cubic interpolations along the thickness might be sufficient to accurately model the mode pattern, thereby leaving the possibility to perform a rather dense mesh along in-plane axes of the plate.

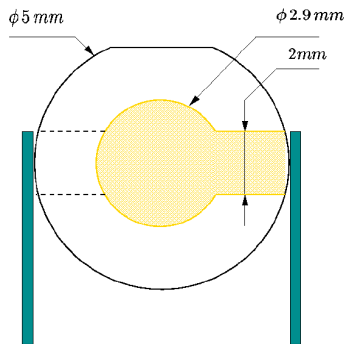


Figure 5-1

Here-presented work was performed with prismatic finite elements with parallelepipedic shape. For such elements, interpolations are cubic along all directions, with incomplete interpolating functions base along in-plane axes and complete one along the thickness.

The mesh of resonator is presented on Fig. 5-2. It contains around 4000 nodes arranged into 420 elements : 228 membrane elements (12 nodes) for the modelling of silver electrodes, and 192 tridimensional elements (48 nodes) for the quartz crystal.

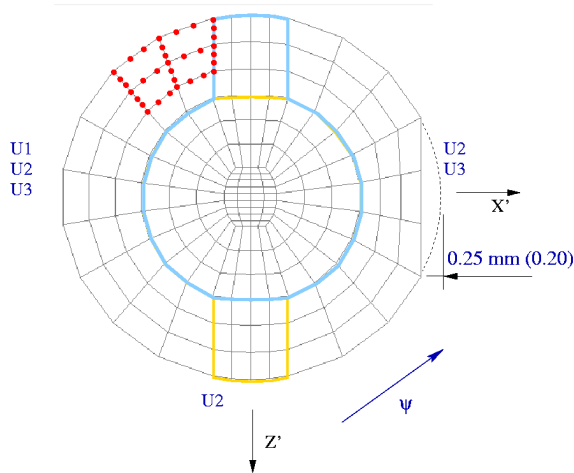


Figure 5-2

With a 550 MHz, rather standard personal computer equipped with 1 giga-byte of memory, analysing this structure requires typically between four and six hours of computation to get thirty modes at a given temperature point.

Our first work consisted in checking the trapping of the mode shape by the mass loading of electrodes deposit. The following values of thickness were tested for silver plating : 58, 80, 100, 120, 140, 160 nm. The theoretical thickness of the quartz plate itself was initially set to 82 μm for the computations and the electrodes tabs were not taken into account at the beginning of this study. Only fundamental B-mode with associated anharmonic responses were modelled. Experimental checking was possible on a few TSQRs made at AE Lab with only 58nm and 180nm plating. In particular, the spectra of two samples were analysed on our X-ray topography system. Obtained mode patterns are produced in [6-1]. The frequency range of FEA-predicted spectrum was in general found significantly more restricted than the range predicted by Tiersten and Stevens analytical model. This was confirmed by experiment. Corresponding data are presented on Table 1. We use the common notations (n,m,p) for mode identification of the mode pattern, where n indicates the overtone number, m the number of nodal planes along X-axis, and p the number of nodal planes along Z' axis. In all cases, FEA results were searched in frequency windows containing 30 eigenmodes. Corresponding columns are not completely filled in here-produced results, and we even did not try to complete them, according to the following discussion:

- We found many abnormalities of the predicted patterns in runs of program performed with rather thick electrode plating. For instance, an additional mode, (1,1,1)-like, is predicted by FEA in case of 180 nm plating. This observation is even reinforced when lowering the plating thickness down to 160 nm. In the case of simulations performed for 100 nm plating, we obtained two slightly perturbed (1,0,0) patterns at 25°C, separated by only 374 Hz. Predicted patterns for $u1$ component are presented on Fig. 6-3. while Fig.5-4 presents the predicted patterns for $u2$. The predicted patterns for $u3$ are quite identical to the ones for $u2$, with relatively comparable amplitude. At different temperatures, for instance 40°C or 10°C, the simulation predicts only one (1,0,0) mode, with a very smooth shape. This is just how FEA predicts activity-dips. In the considered case, examining the patterns of Fig 5-4

shows that the main component u_1 is coupled with combined face shear and flexure wave travelling along Z' direction.

From another hand, X-Rays topography presented in Fig.6-14 to 6-17(chapter 6) of the companion paper for the thicker plating show a strong offcentering and a $\pi/4$ rotation of the mode shape which could not be explained by introducing a defect of parallelism of the quartz plate in finite element analysis, for instance. At the same time, introducing such defect in simulations for 58 nm plating improved the realism of simulations, as can be observed when comparing Fig. 4-5 (defect 0.5% between centre and the circumference of plate in X-direction) with Figs. 8-11of [6-1]. Distortion of topography obtained for (110) and (102) modes (Figs. 5-6 of Ref. 4) are left over from such comparison because of the actually high level of drive used during X-ray analysis: in case of resonant modes with very close frequencies, the actual response does not come from a single eigenmode.

Combining our feeling of better understanding of the behaviour of the 58 nm-plated sample and the prediction of many activity dips for designs with thicker plating, we decided to pursue the systematic analysis of the influence of construction parameters with a thickness of plating fixed to 58 nm. For this case, the second FEA column in Table I was obtained when taking into accounts electrode tabs in the FEA model. It is worth remarking that this change was sufficient to modify the ordering of the close modes labelled (110) and (102) making it conforms to the measured order. This confirms the importance of electrode tabs previously asserted at [4-3].

Plating 180 nm				
$f-f_{100}$ (kHz)				
mode	Tiersten	FEA		Measured
1,0,1	44	24		39
1,0,2	134	59		61
1,1,0	144	61		-
1,1,1	189	97		154
1,0,3	267	107		
1,1,2	278			
1,1,3	411			
1,2,0	421			
1,0,4	440			
1,2,1	466			
Plating 58 nm				
$f-f_{100}$ (kHz)				
mode	Tierste	FEA		Measured
1,0,1	42	23	22	21
1,0,2	123	55	53.7	46
1,1,0	125	54	54	52
1,1,1	-	87	87	79
1,0,3	-	98	94	92
1,1,2	-	128		119
1,2,0	-	137		125
1,0,4	-	150		138
1,2,1	-			168

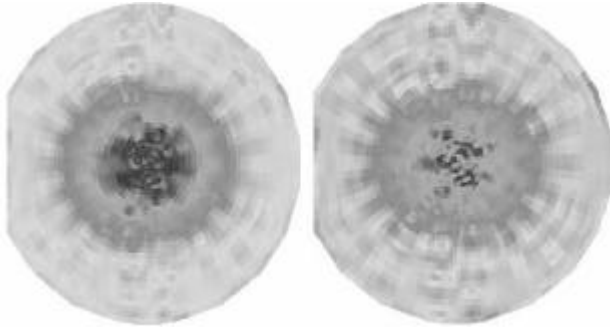


Figure 5-3

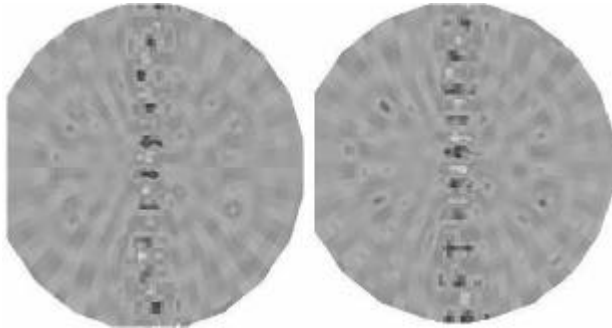


Figure 5-4

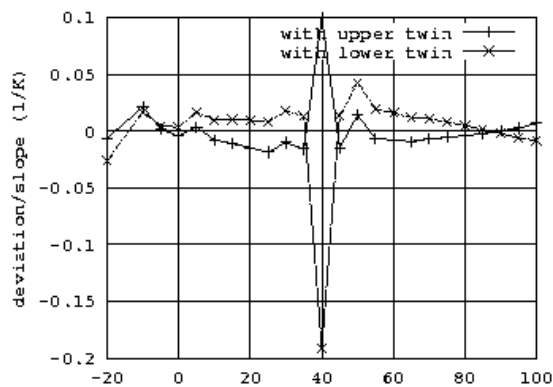


Figure 5-5

To more precisely investigate the influence of tabs, we simulated by FEA the frequency temperature characteristics of TSQR by 10°C increment between 20°C and 100°C. This was intended for the design with electrode tabs and silver plating 58 nm thick, upon rotating the material constants around the plate normal by the following angles : $\psi=0, \pi/8, \pi/4, 3\pi/8, \pi/2, 5\pi/8, 3\pi/4, 7\pi/8$. Only the values of ψ in the range $[0- \pi/2]$ have been checked yet. Nevertheless, it was found that rotating the whole shape of resonator has definite impact on the occurrence of activity-dips. For instance,

with $\psi=0$, the simulation predicted a splitting of (1,0,0) mode at 40°C. With $\psi = \pi/8$, the same kind of splitting occurred at 60°C, and, with $\psi=3\pi/4$, such incident was predicted at 70°C. At first sight, these cases seem to concern the *same* activity-dip, continuously affected by the rotation of the design around its own normal. We intend to confirm this by a more refined analysis with smaller steps for ψ and for the temperature. We have previously proposed at [5-2] a method to quantitatively appreciate the strength of the dip: it consists of plotting the deviation between the actual frequency-temperature characteristic and a cubic fit of it. When the mode of interest splits in two twin modes under the action of thermo-dependent coupling, the frequencies of the twins are symmetrically located below and above the frequency predicted by the least cubic fit. We present such a typical situation on Fig. 5-6, for the case of the predicted dip at 40°C and $\psi=0$, which yields two (1,0,0)-like mode patterns represented on Fig. 5-7, separated by only 330 Hz.

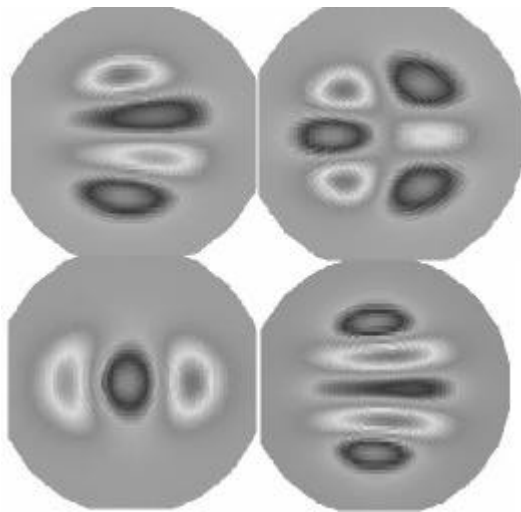


Figure 5-6

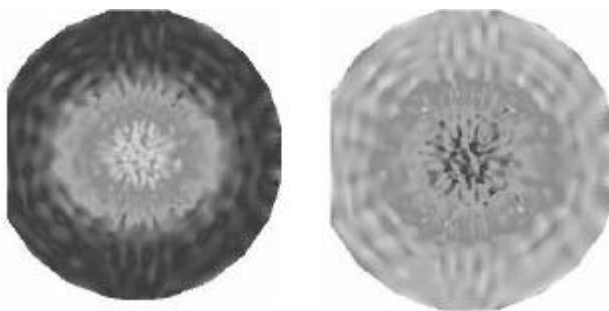


Figure 5-7

Farther, a perturbation of (1,0,0) mode was predicted only at 100°C with $\psi=3\pi/4$, but this perturbation was very slight, and, at the end, only the +40°C point corresponded to very slight defect of smoothness of the mode pattern with $\psi=\pi/2$. It was not possible to relate those temperature-dependent perturbations with already investigated ones, due to the noisy character of simulations for u_2 and u_3 minor components of the mode. It must be recalled that the proper identification of activity dip caused by high order harmonics of flexure or face shear waves may imply the use of a specific finite element mesh, depending on the number of oscillations of the spurious mode

concerned. Other clues of activity-dips were found acting on anharmonic modes such (1,0,1) and (1,0,2), (1,0,3) for various parameters.

On previous results of simulations, the distance between the flat and the circumference of the was set equal to 0.25 mm. After setting it equal to 0.20 mm we got a clear perturbation of (1,0,0) mode at 60°C on the frequency-temperature characteristic by 10°C steps. Interestingly enough, at 70°C the (1,0,0) mode pattern became smooth, while the (1,0,1) became perturbed, but the patterns obtained for the minor components of the vibration are still too noisy to estimate if both perturbations come from the same kind of spurious mode, not so temperature sensitive and crossed by the successive thickness modes which all exhibit temperature sensitivities near – 1000Hz/ for this design. At this moment, the steps used for parameters changes are still a bit large to allow for such a continuous tracking of the activity dips. Nevertheless, it is common situation to observe that a neighbouring anharmonic mode becomes perturbed instead a previous one after a change of parameter. For the class of here-studied resonator, we estimate that temperature steps of 2.5°C may be sufficient to accurately follow the continuous evolution of activity dips along most of geometrical parameters changes considered here.

We performed also other simulations, still for the case of 58 nm plating and with electrode tabs, together with flat-to-circumference distance set equal to 0.25 mm, but with electrodes diameters decreased to 2.4, 2.0 and 1.6 mm. Temperature-dependent perturbations were still predicted, but could not be connected with previously investigated ones. By the way, diminishing electrode diameter by 0.5 or 0.4 mm is a big change, as can be checked on Fig. 5-8, showing the mode pattern at 40°C for the main mode and electrode diameter equal to 2.0 mm. The effect of tabs is comparatively reinforced by the reduction of electrode diameter, so that the vibration is much less trapped along the tab orientation (vertical on the picture). This involves some change of the spectrum and mode shape of higher anharmonic modes, making the analysis difficult to compare with previously presented ones.

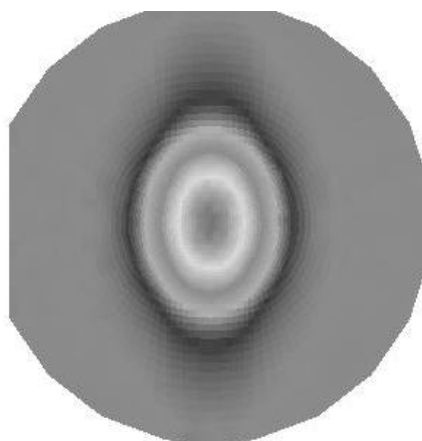


Figure 5-8

6. X-RAY THOPOGRAPHY OF NLC-CUT TSQR

We have used X-Ray topography to investigate the resonant frequencies and mode shapes in 29,3 MHz resonators.[6-1] Due to the fact that the resonant frequencies of quartz are, of course, very sensitive to change of temperature, and because we want to

observe very leak resonant modes, a real time control of mechanical resonance by X Ray diffraction is needed. It is the reason for which we didn't use the Lang experiment setup. Instead of we have used a large focus X-Ray tube to illuminate the quartz crystal, and an image intensifier to obtain a real time visualization of the diffracted image. Since we don't need a very high resolution the record of the diffracted beam can be. made on high speed photographic film.

6.1. Experiment

The construction parameters of the quartz resonators are:

diameter of quartz plate : 5 mm
 thickness of quartz plate: 82 μm
 diameter of electrodes: 2.9 mm
 width of electrode tabs: 1 mm

The direction of X crystallographic axis is perpendicular to the flat made on the plate (see figure 6-1).

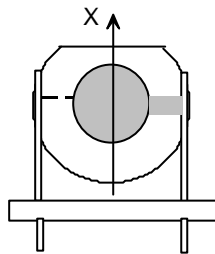


Figure 6-1

Two groups of quartz having different thickness have been studied.

7.2 Results

1. Resonator with electrode thickness 58 nm

The figure 6-2 show the module of admittance of a resonator. Vertical unit is in dB, with a zero level corresponding to 10.5 Ω

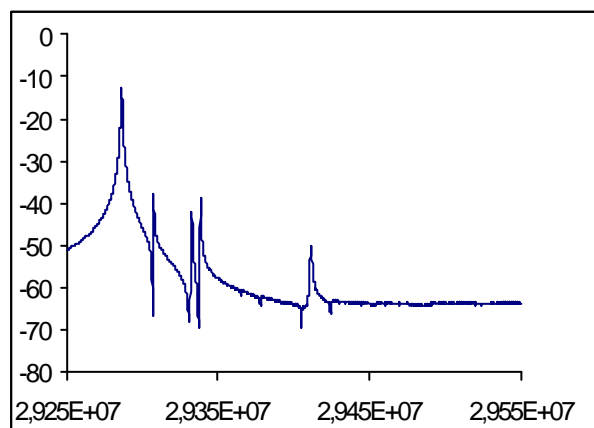
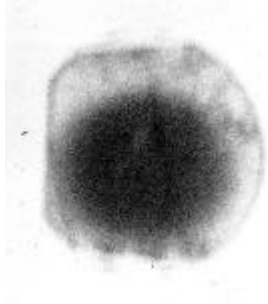


Figure 6-2

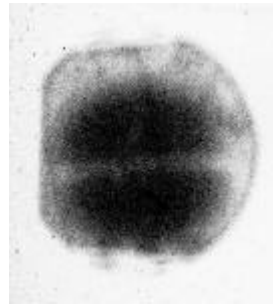
Aside the four active spurious mode, there exist five other “disturbances” corresponding to modes that are observable by X-Ray imaging. In this resonator the

trapping of the vibration is not very strong. As expected from the Tiersten theory of energy trapping in singly rotated resonators [6-3], the nodal lines are in the X and Z' direction. The X axis is oriented in the horizontal direction. The topographies are made at room temperature.



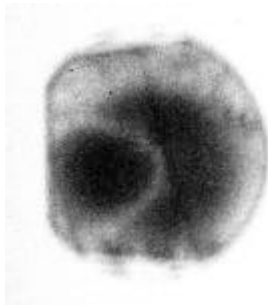
f=29.286 MHz

Figure 6-3



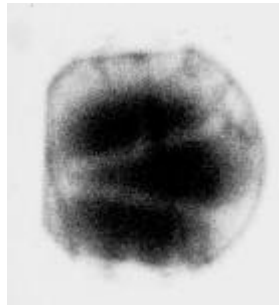
f=29.307 MHz

Figure 6-4



f= 29.332 MHz

Figure 6-5



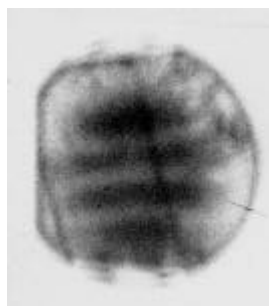
f=29.338 MHz

Figure 6-6



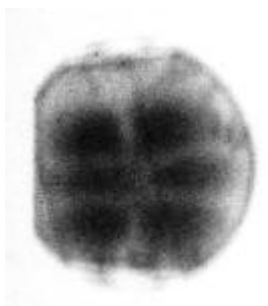
f=29.365 MHz

Figure 6-7



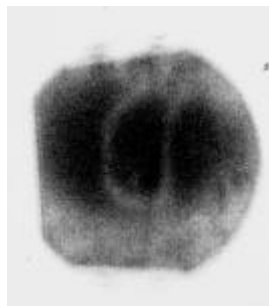
f=29.378 MHz

Figure 6-8



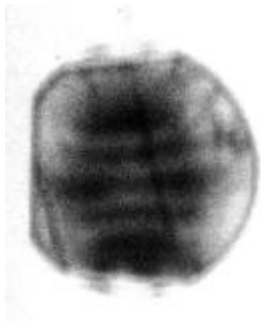
f=29.405 MHz

Figure 6-9

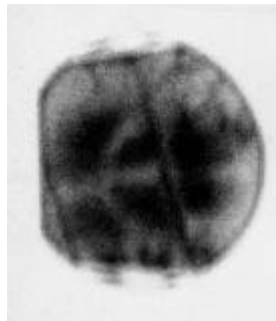


f=29.411 MHz

Figure 6-10



f=29.424 MHz



f=29.454 MHz

Figure 6-11

Figure 6-12

The mode on figure 6-3 is the main mode on which the thermal sensor operates. The pictures on figures 6-4,6-5,6-6 and 6-10 are for the principal spurious resonances. The unusual shape of 1,1,0 mode in figure 6-5 comes from the superposition of this mode with the 1,0,2 mode (Fig 6-6) because both modes have very close resonant frequencies.

3.2 Resonator with electrode thickness 180 nm

The “frequency spectrum” of a typical resonator is shown on figure 6-13.

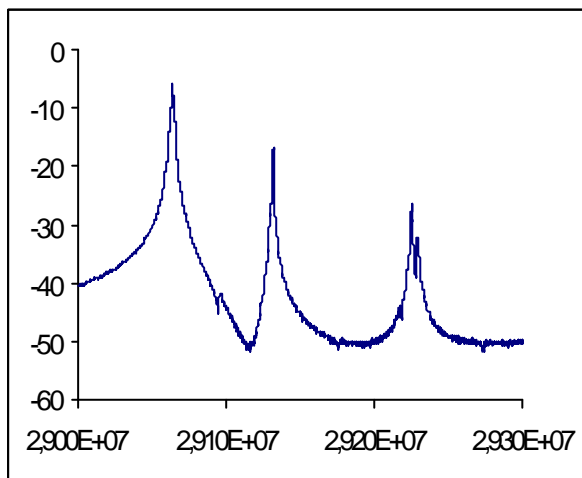


Figure 6-13

On all topographies (Fig.6-14 to 6-17), the component of the mechanical displacement the diffraction is sensitive lies in the horizontal direction. Since the trapping of the vibration is strong in this resonator, spurious modes are more spaced and less numerous than in the first group of resonators.

The figures 6-14 to 6-15 give the mode shape of the main mode and of the first two anharmonic modes. The u_1 component along X axis the mechanical vibration is depicted on the left part of the figures (use 2-1.0 reticular plane), while the u_3 component along Z' axis is on the right (use of 0 0.1 plane). We observe that the nodal lines of the mode shapes are not in the expected direction. The origin of this

rotation of mode shape is not well understood for instance. A possible explanation is an effect coming from a lack of parallelism of the plate[6-3,6-4]. The similarity of the topographies showing the u1 and the u3 component of the vibration seems to indicate that the mechanical displacement is not exactly along the X direction.

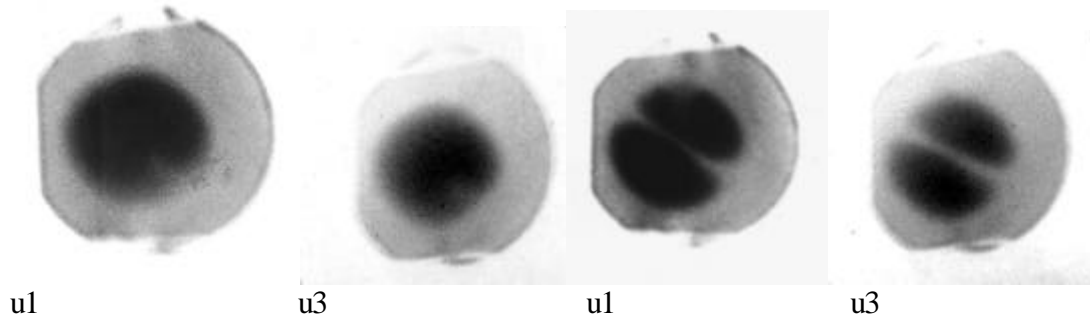


Figure 6-14 f=29.071 MHz

Figure 6-15 f=29.110 MHz

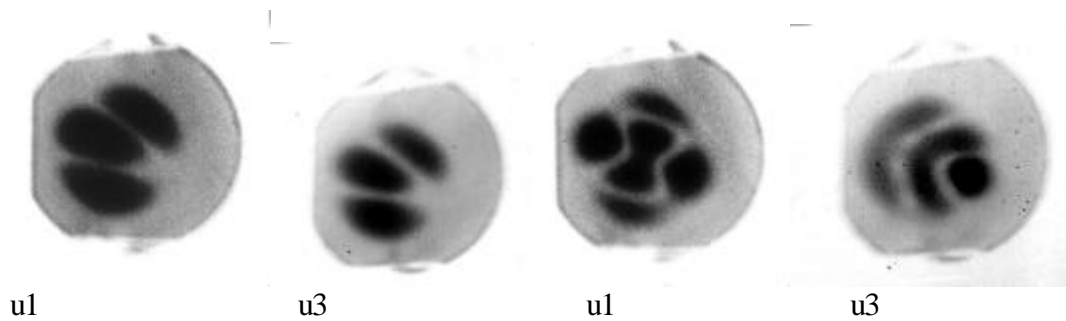


Figure 6-16 f=29.132 MHz

Figure 6-17 f=29.225 MHz

The complex mode shape shown on figure 6-17 corresponds to the three close spurious resonances on the right side of record on figure 6-13 and is a mixing of three “normal” anharmonic modes. In this last case, the u1 and the u3 component of the vibration exhibit different distribution.

All mode shapes shown on the topographies are not exactly centered and the deformation of the mode shapes can be explained by a small defect of parallelism of the faces of the resonator, as it can be verified by fem analysis.[6-5]

7. RADIATION RESISTANCE OF THERMOSENSITIVE QUARTZ CRYSTAL RESONATORS

Thermosensitive quartz crystal resonators were irradiated by gamma Cobalt60 source and by fast neutrons from Pulsed Neutron Reactor. Resonators are realized on flat parallel quartz plates, $yxbl/10\ 54/11\ 06'$ crystalline cut operate at 26.5 MHz on 3-td overtone and thickness shear C-mode.

It has been measured frequency as function of radiation dose at different temperatures. The offset of temperature frequency characteristic of TSQRs under irradiation of fast neutrons up to 2.10^{14} n/cm² and gamma rays up to 5 MRad are investigated.

Radiation resistance of thermosensitive quartz crystal resonators (TSQRs) is important factor for their application for cryogenic temperature measurement under neutron fluence and gamma environment. To clarify their radiation resistance TSQRs were irradiated by gamma Cobalt60 source and by fast neutrons from Pulsed Neutron Reactor. Neutron radiation was carried out at liquid nitrogen and room temperature and gamma radiation only at room temperature.

Cultured Z-growth quartz with up to 30ppm of aluminum and 10ppm of sodium and lithium content has been used. The induced effects of ionizing radiation on quartz crystal resonators can be discussed in terms of a model of one of the primary impurity defects in quartz. This defect is substitutional Al^{3+} defect with an associated interstitial charge compensator, either a H^+ , Cl^+ , Na^+ ion or a hole.

Quartz is grown in an alkali-rich environment and lithium and sodium are trapped interstitially next to the aluminum with the valence electron providing the compensation. The sodium sit off the X-axis in the Z-axis channel; and the resulting Al-Na center causes a strong acoustic loss peak at 53K and a much weaker peak at 135K. Lithium, however, sits on the X-axis and consequently, the Al-Li center shows neither acoustic nor dielectric loss peaks. [7-1]

Martin et al.[7-1] discussed the conversion by irradiation of the Al-Li (and Al-Na) centers into a mixture of Al-OH center does not produce an acoustic loss peak. However, acoustic loss peaks at 23K, 100K and 135K are associated with the presence of the Al-hole center.

Changes in the elastic constants of the crystalline structure, besides causing obvious frequency changes, will also cause changes in the frequency-temperature characteristics of the quartz resonator.

7.1. Experiment

The irradiation by gamma rays from Cobalt 60 with intensity of 0,459 kGy/h was carried out at room temperature at INRNE, BAS, Bulgaria. The resonant frequency of TSQRs before and after irradiation at temperature 273K, was measured by step 1MRad. Frequency measurement was made after each dose radiation. Uncertainty of measurement is about $\pm 1 \cdot 10^{-6}$. The temperature 273K is provided by mixture of ice and water in ratio 2:3 with accuracy of $\pm 0,01K$. Temperature gradient in Dewar is not more than 0,01K/cm.[7-2]

The irradiation by fast neutrons has been carry out at the pulsed neutron reactor IBR-2, Laboratory of Nuclear Physics, JINR, Dubna, Russia. It produced a full spectrum of fast neutron ranging from $10^{-1}MeV$ to 20MeV; average energy $E_n \approx 1MeV$. The reactor can deliver the neutron flux up to $10^{12}n/cm^2$ over areas up to 20x40cm.

In addition to the neutron, gamma radiation is also produced in the nuclear reaction with maximal dose rates up to 10Gy/s. The average energy is about $E_\gamma \approx 1,5MeV$. The flux of the fast neutrons of $10^7 - 10^8 n/cm^2 \cdot sec$ was used for our measurements.

The experimental setup[7-2] includes a cryostat for the sensors, nickel foil for both - monitoring of the total reactor power and measuring of the homogeneity of the neutron fluence. The induced activity in this foil was used for monitoring of the total reactor power. To monitor the dose rates, the neutron and gamma dosimeters were mounted around the cryostat. The accuracy to determine the fluence of the fast neutrons and γ -dose was $\pm 10\%$. [7-2]

The main interest on this setup is its ability to monitor on-line the evolution of the TSQRs by comparing their readout with temperature references that are in principle insensitive to the neutron irradiation.

Setup of measurement of frequency and resistance is shown on Figure 7-1.

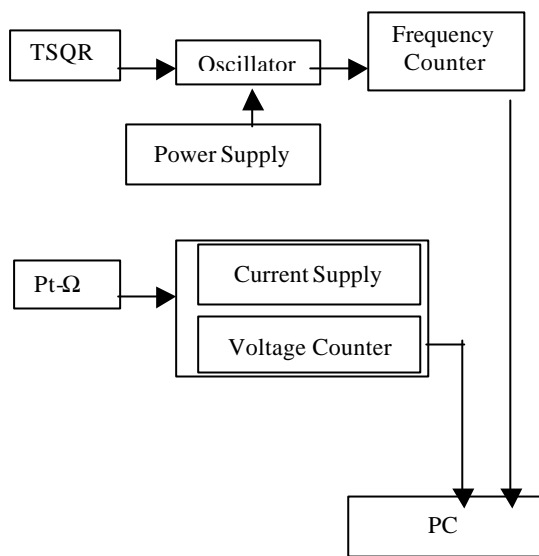


Figure 7-1.

A high-frequency matching cable to the measuring oscillator connected the quartz thermosensitive resonator. The frequency was measured by a $\times 3-64$ frequency counter with uncertainty about of $\pm 1,10^{-9}$. The temperature and frequency data are read every second by the personal computer (PC), where they are displayed as graphics and saved in files.

7.2. Results

7.2.1. Gamma radiation

We have measured frequency-temperature curves as functions of radiation dose after each dose gamma rays: 1MRad, 2MRad, 3MRad, 5MRad. Two groups of resonators are irradiated - one with good frequency-temperature characteristic (TFC) and second with bad TFC. Good TFC means that the resonator have smooth TFC without interruption and break of frequency over temperature range from 77K (temperature of liquid nitrogen) to 300K (room temperature). Bad TFC means that the resonator has a lot of interruptions, breaks and its TFC is not smooth.

Investigations show reduction of frequency up to 3MRad dose gamma radiation. The frequency depends on gamma dose nonlinearly. There is high frequency shift at low doses up to 3MRad and very small frequency shift at high gamma doses up to 5MRad. There is a saturation of frequency shift after dose 3MRad. Up to the 1MRad the frequency shift is positive. It is due to the carrying out of relaxation process, surface strain, adsorption, absorption, dissociation, and polymerization or relaxation effect in electrodes and crystal holders.

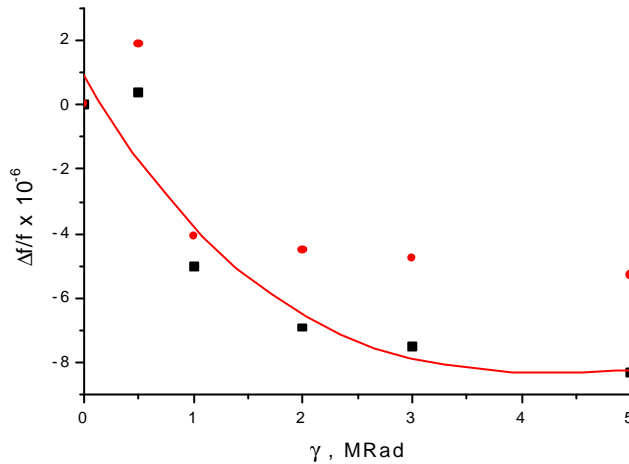


Figure 7-2

7.2.2. Neutron radiation

We have measured frequency-temperature curves as functions of radiation dose at different temperatures and at different intensity of neutron beam.

Three groups of TSQRs and Platinum resistance sensors were irradiated with the gamma rate 23kRad and neutron flux of 10^{13} - 10^{14} n/cm² at room and liquid nitrogen temperatures.

The first group of sensors was putted in liquid nitrogen during irradiation to dose $3,8 \cdot 10^{13}$ n/cm². The second group was mounted on the air close by cryostat where intensity of neutron beam is $7 \cdot 10^7$ n/cm².sec to dose $5,8 \cdot 10^{13}$ n/cm². The third group was mounted on the air, near to center of the neutron beam, where its intensity is $1,9 \cdot 10^8$ n/cm².sec to the dose $1,6 \cdot 10^{14}$ n/cm².

At the beginning we measured temperature-frequency characteristic of TSQRs and after that the pre- and post- irradiation comparison was made. TSQRs have exhibited the frequency shift $\Delta f/f$ about $1,2 \cdot 10^{-6}$ during neutron plus gamma radiation doses up to 10^{14} n/cm², $E_n > 100$ keV and $2 \cdot 10^3$ Gy, $E_\gamma \approx 1,5$ MeV at 77,4K and $\Delta f/f$ about $9 \cdot 10^{-6}$ at 300K. These values are within the accuracy of their calibration characteristics and within uncertainty of measurements.

During the test the TSQRs and reference sensors were immersed in the Dewar with liquid nitrogen whose level was kept constant with deviation of ± 5 mm at the moment of measurement. To avoid the influence of oxygen concentration on saturated pressure of liquid nitrogen, the fresh nitrogen was transferred into the cryostat from the laboratory 1000l storage vessel to minimize contamination. For the presented data the problem with dissolved oxygen were neglected. [7-2, 7-3]

7.2.3. Frequency correction procedure

As we want to estimate the irradiation induced frequency offset of our sensors, we must ignore the frequency changes due to the temperature drift. This is done with the following correction procedure:

- 1) We choose a correction temperature – 77,35K in liquid nitrogen and 290,73K on air.
- 2) Rejected points – all the points outside the range $[77,35 \pm 0,01]$ K at liquid nitrogen and $[290,73 \pm 0,2]$ K on air.

- 3) For each measured point we calculated $\Delta F = F_{\text{measured}} - F_{\text{correction}}$
- 4) We obtain: $T_{\text{correct}} = T_{\text{measured}} \pm \Delta T(dF/dT)$ where dF/dT is temperature sensitivity of the sensor.

Figure 7-3 shows frequency shift of TSQR at liquid nitrogen temperature. Stability of the temperature is $\pm 0,01\text{K}$ which corresponding to frequency shift $\Delta f/f$ about $\pm 1,3 \cdot 10^{-6}$, and in our case we obtained $\Delta f/f$ about $1,2 \cdot 10^{-6}$. This result shows that the frequency shift of TSQR due to irradiation by fast neutrons is in the limits of temperature instability of resonators.

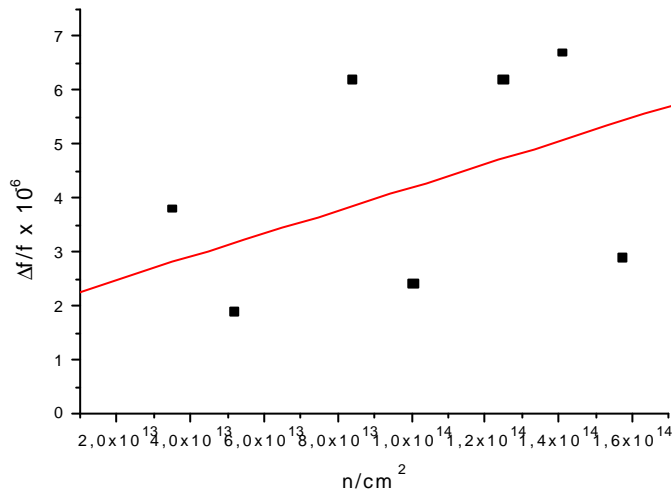


Figure 7-3

The Figures 7-4 and 7-5 show that frequency shift of TSQRs is the same at different intensity of neutron beam at room temperature.

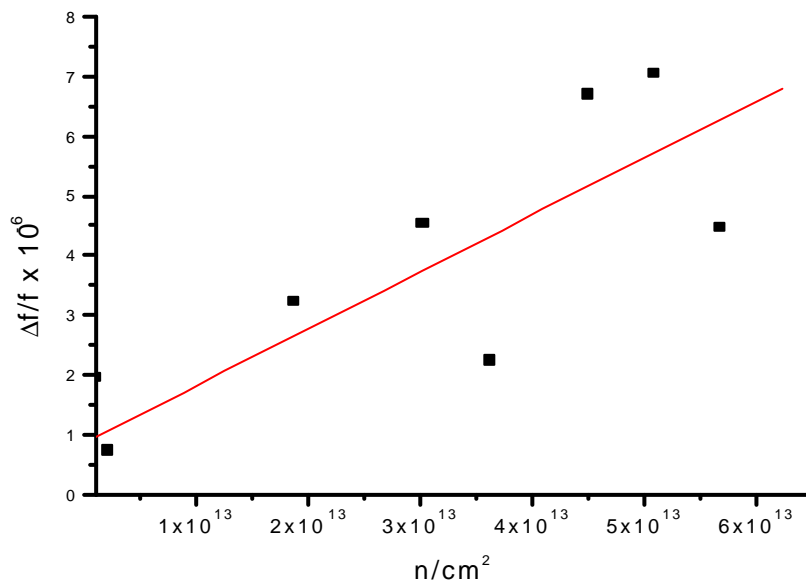


Figure 7-4

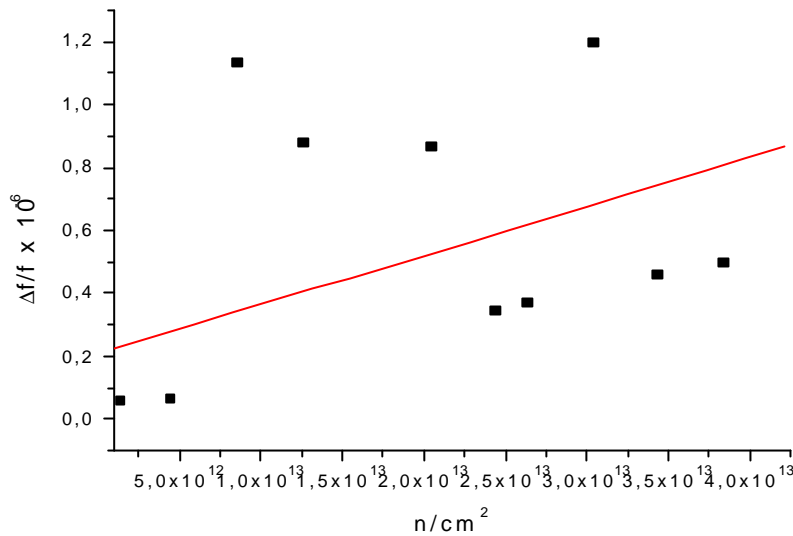


Figure 7-5

8. INFLUENCE OF MAGNETIC FIELD ON TEMPERATURE FREQUENCY CHARACTERISTIC OF TSQR

Systems to measure temperatures of superconducting installations require exact and reliable cryogenic thermometers. We have investigated influence of the magnetic fields up to 5 T on the temperature-frequency characteristics of the thermal-sensitive quartz crystal resonators (TSQR) and TVO-resistors used as temperature sensors. The experimental set-up and procedures are described, and experimental results are presented and discussed as well.

We have used a solenoid superconducting magnet consisting of two coaxial sections which allows one to change the temperatures within its volume. A cryostat is filled with liquid helium, and the temperatures can be regulated within the range from 4K to 5K.

Thermal-sensitive quartz crystal resonators possess temperature sensitivity of 1000Hz/K at the temperature range from 130K to 450K, however its sensitivity is 2Hz/K only at the temperature of liquid helium. Experiments have shown that the readings of TSQR-sensors practically do not depend on the magnetic field, and these sensors are able to provide reliable routine measurements of temperatures in physical and industrial installations under condition combining magnetic field up to 5T and cryogenic temperatures. The resistance of the TVO-sensors increases due to the magnetic field by several percent. However, the important feature of the TVO-sensors is that their behavior under magnetic fields is predictable with the deviation about ± 0.02 K [8-1,8-2,8-3].

Thermosensitive quartz crystal resonators are realized on quartz plate $yxbl/10^\circ 54'/11^\circ 06'$ – cut. TSQRs were made by Acoustoelectronic laboratory of Institute of Solid State Physics, Bulgarian Academy of Science and experiment of influence of magnetic field at Joint Institute for Nuclear Research, Dubna, Russia.

There is a carbon resistive temperature sensor based on the TVO resistor among the TSQRs. Physical configuration is a rectangular prism of 8mm length and 1,3x2,4 mm² cross-section with two cooper leads. It has ceramic and glass coats to provide a hermetic seal, and can be used in the environment combining moisture, corrosion, vibration, high and low temperatures.[8-3] This sensor is suitable for routine measurements in the high magnetic field because its behavior in magnetic fields can be predicted.[8-1,8-2,8-3]

8.1. Experiment

We use a solenoid superconducting magnet, which consist of two coaxial sections. The dimensions of magnet are follows: height - 0,22 m, inner diameter - 0,038 m, outer diameter - 0,27 m. The maximum field in the center of the solenoid is 5T at 4,2K to 4,6K. The solenoid is supplied by a stabilized current source(U=6 V, I=70 A). Its integrator provides a smooth input/output of the current with the speed up to 0,5 A/s. The LMK Hall sensor is used to measure the magnetic field.

Cryostat is filled with liquid helium and the temperature can be regulated within the range from 4,2 K to 4,6 K. Magnetic field- independent temperature control was accomplished with the system to keep the pressure at the given value and measure the corresponding vapor pressure of the used cryogen.[8-2]

Experimental setup is shown on Figure 8-1, where 1 is removable maintenance, 2 - changeable concentrator of magnetic field, 3 - Hall sensor, 5 - reference thermometer, 6 - plate on which situated TSQRs - 4, 7 - solenoide, 8 - sistem of measurement.

Magnetic field is changed from 0 T to 5 T, along this temperature of liquid helium is changed from 4,2 K to 4,6 K.

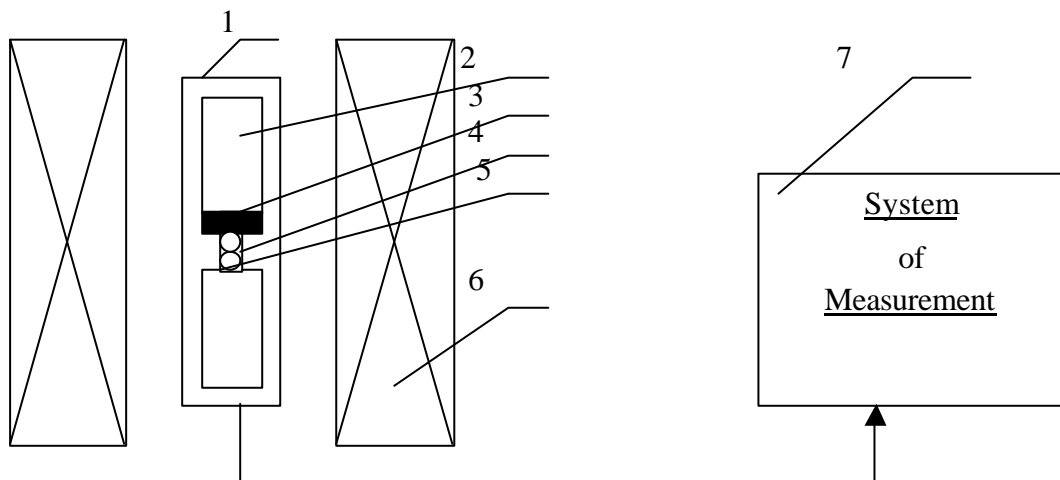


Figure 8-1

We have made calibration of TSQRs and TVO resistors before putting them in the magnetic field.

Orientation of quartz plate with respect to magnetic field is shown on Figure 8-2.

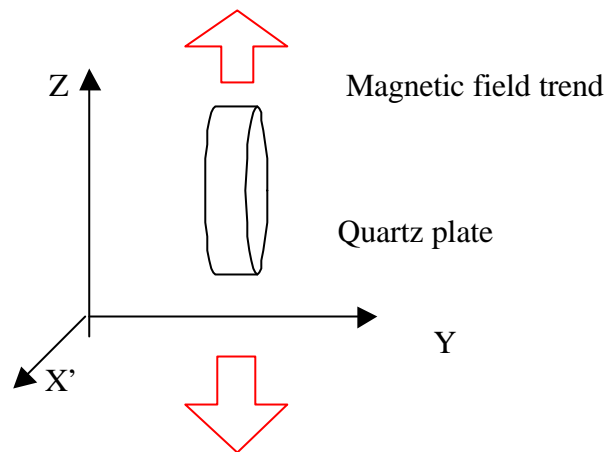


Figure 8-2

8.2. Results

At the beginning we measured a frequency of TSQRs without magnetic field and next we began measuring during increasing and decreasing of magnetic field by step of 1T. Figure 8-3 shows frequency shift versus magnetic field at different temperatures. We have measured frequency shift of TSQRs with respect to magnetic field at 4,2 K; 4,4 K and 4,6K.

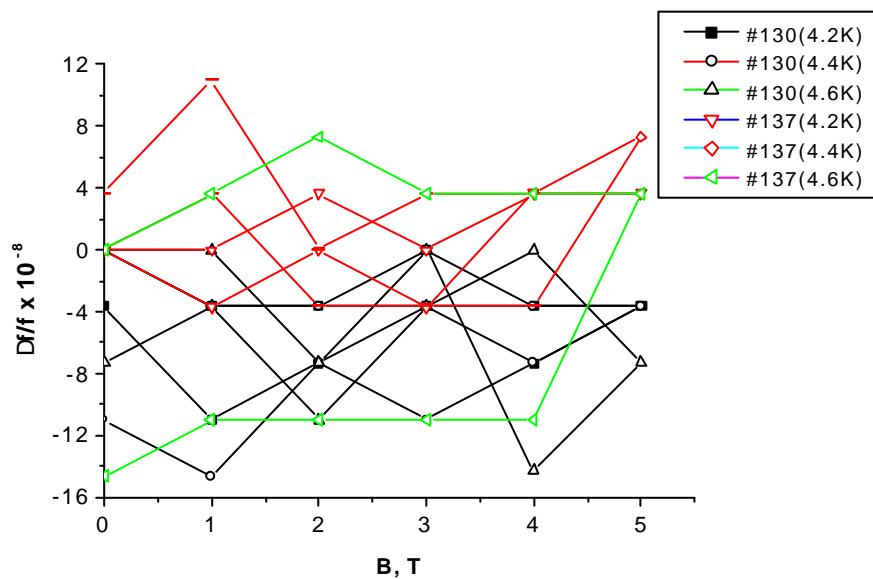


Figure 8-3

The results has shown that frequency shift $\Delta f/f$ is about $15 \cdot 10^{-8}$ at temperatures 4,2 K; 4,4 K and 4,6 K, which is in uncertainty of measurement. This allows the using of TSQR as reliable temperature sensors working under magnetic field up to 5 T.

9.CONCLISION

1. Review on different kind of influences on quartz resonators characteristics is studied.
 2. Temperature-frequency characteristics of thermosensitive quartz resonators with different kind of cuts are investigated in wide temperature interval. The selection method and calibration methodology of platinum resistance thermometers and thermosensitive quartz resonators (TSQR) are created.
 3. Investigation of the influence of the cryogenic temperatures on temperature frequency characteristic of TSQR is made. Some disturbances are appeared at temperature range [90-110] K and [120-135] K. These disturbances are due to possible acoustic coupling between main and spurious modes, which have different temperature dependence. This phenomenon is called "activity dips".
 4. The X-ray topography of the resonators was carried out, which prove existed "activity dips"
 5. Influence of radiation environment (gamma rays and fast neutron) and magnetic field was investigated. The experiments show that there is a frequency shift of $-8 \cdot 10^{-6}$ after gamma dose of 5MRad, but there is not frequency shift after neutron irradiation of 10^{14} n/cm².
- One can conclude that the thermosensitive quartz crystal resonators can be used as reliable temperature sensors working under above-mentioned conditions.

LIST OF PUBLICATIONS RELATED TO PhD THESIS

1. V. Georgiev, L.Spassev, L. Vergov, **R. Velcheva**, "Some Investigations of Thermosensitive Quartz Crystal Resonators at Cryogenic Temperatures", 14th European Frequency and Time Forum, pp. 273-275, Torino, 2000
2. B. Dulmet, R. Bourquin, L. Spassev, V. Georgiev, **R. Velcheva**, "Investigation of Activity-Dips in Thermo-Sensitive Quartz Resonators at Cryogenic Temperature", 15th European Frequency and Time Forum, pp.79-83, Neuchatel, 2001
3. **R. Velcheva**, L. Spassev, V. Datskov, V. Drobin, L. Petrova, "Precise calibration of stable temperature sensors", 11-th International Symposium "Metrology and Metrological Assurance", pp. 44-49, Sozopol, 2001
4. **R. Velcheva**, L. Spassev, Yu. Filippov, V. Miklayev, V. Shabratov, "Influence of Magnetic Field on the Frequency Response of the Thermosensitive Quartz Crystal Resonators", The 6th International Workshop "Relativistic Nuclear Physics from HUNDREDS of MeV to TeV", Varna,2001, in press
5. **R. Velcheva**, Yu. Filippov, L. Spassev, E. Kulagin, N. Agapov, "Reactor Irradiation on Thermal-Sensitive Quartz Crystal Resonators", The 6th International Workshop "Relativistic Nuclear Physics from HUNDREDS of MeV to TeV", Varna,2001, in press
6. B.Dulmet, R.Bourquin, L.Spassev, **R.Velcheva**, Finit Element Analysis of Activity Dips in NLC-cut Quartz Temperature Sensors, pp.D_033, Proc. Of 16th European Frequency and Time Forum, 2002
7. R.Bourquin, B.Dulmet, L.Spassev, **R.Velcheva**, Study if NLC-cut Resonators by X-ray Topography, pp. D_60, Proc. Of 16th European Frequency and Time Forum, 2002

8. L.Spassev, **R.Velcheva**, Ts.Yordanov, L.Vergov, B.Dulmet, R.Bourquin, Investigations of Thermosensitive Quartz Resonators NLC-cut at Cryogenic Temperatures, pp.D_037, Proc. Of 16th European Frequency and Time Forum, 2002
9. **R.Velcheva**, L.Spassev, Yu. Filippov, E. Kulagin, V. Miklayev, Radiation Resistance of Thermosensitive Quartz Crystal Resonators, pp.D_048, Proc. Of 16th European Frequency and Time Forum, 2002
10. **R.Velcheva**, L.Spassev, Yu.Filippov, E.Kulagin, V.Miklayev, Thermosensitive Quartz Crystal resonators under radiation environment, *Nuclear Instrument and Methods – Section B*, under revision
11. **R.Velcheva**, Ts.Yordanov, L.Spassev, Yu.Filippov, Thermosensitive Quartz Resonators NLC-cut as Temperature Sensors, *Sensors & Actuators*, under revision

REFERENCES

- [3-1] E.Benes, M.Grosch, W.Burger, M Schmid, “Sensors based on piezoelectric resonators”, *Sensors and Actuators A*, 48, pp1-21, 1995
- [3-2] L.Spassev, V.Georgiev, L.Vergov, N.Vladimirova, V.Drobin, N.Agapov, Thermosensitive Quartz Crystal Resonators at Cryogenic Temperatures, *Sensors and Actuators A*, vol.62, pp.484-487, 1997
- [3-3] V. Georgiev, L.Spassev, L. Vergov, R. Velcheva, “Some Investigations of Thermosensitive Quartz Crystal Resonators at Cryogenic Temperatures”, 14th European Frequency and Time Forum, pp. 273-275, Torino, 2000
- [4-1] B. Dulmet, R. Bourquin, L. Spassev, V. Georgiev, R. Velcheva, “Investigation of Activity-Dips in Thermo-Sensitive Quartz Resonators at Cryogenic Temperature”, 15th European Frequency and Time Forum, pp.79-83, Neuchatel, 2001
- [5-1] B.Dulmet, R.Bourquin, L.Spassev, R.Velcheva, Finite Element Analysis of Activity Dips in NLC-cut Quartz Temperature Sensors, Proc. of 14th European Frequency and Time Forum, 2002
- [5-2] D.C.Zienkiewicz, *The Finit Element Method*, Ed.Mac Graw Hill, 1977
- [5-3] G.Dhatt, G.Touzot, *A Presentation of Finite Element Method*, Ed Maloine S.A., Paris, 1984
- [8-1] R.Bouquin, B.Dulmet, R.Velcheva, L.Spassev, Study of NLC-cut Resonators by X-ray Topography, Proc. 16th Ann. Freq.Control Symposium, S.Petersburg, 2002, in press
- [8-2] R.Bourquin, B.Dulmet, G.Genestier, Jumps in Frequency Temperature Response of Countered Resonators: An Analysis Performed with a Perturbation Model and X-ray Topography, *IEEE Ultrasonic Symposium*, pp.394, 1984
- [7-1] J.Martin, Radiation-Induced Frequency Offsets and Acoustic Loss in AT-cut Quartz Crystals, *Journal of Applied Physics*, vo.68, no10, pp.5095, 1990
- [7-2] R. Velcheva, Yu. Filippov, L. Spassev, E. Kulagin, N. Agapov, “Reactor Irradiation on Thermal-Sensitive Quartz Crystal Resonators”, *The 6th International*

Workshop “Relativistic Nuclear Physics from HUNDREDS of MeV to TeV”, Varna, 2001, in press

[7-3] R.Velcheva, L.Spassev, Yu. Filippov, E. Kulagin, V. Miklayev, Radiation Resistance of Thermosensitive Quartz Crystal Resonators, Proc. Of 16th European Frequency and Time Forum, 2002, in press

[8-1] R.Velcheva, L.Spassev, Yu.Filippov et al, Influence of Magnetic Field on Frequency Response of the Thermosensitive Quartz Crystal Resonators, 6th International Workshop of Relativistic Physics from hundred of MeV to TeV, Varna, Bulgaria, 2001

[8-2] Miklayev V. et al, Behavior of the TVO Temperature Sensors in Magnetic Fields, Particle and Nuclei Letters, No.4[101], 2000

[8-3] Yu.Dedocov et al, Characteristic of Russian Cryogenic Temperature Sensors under Magnetic Fields, HEACC 2001, Japan 2001

[8-4] Yu.Filippov, V.G.Shabratov, Measurement of Helium Temperatures by TVO-sensors under Magnetic Fields, Cryogenics, vol. 42, pp.127-131, 2002